Nuclear Instruments and Methods in Physics Research A291 (1990) 481–486
North-Holland

EMITTANCE MEASUREMENTS OF CESR USING THE EMITTED RADIATION FROM A SHORT-PERIOD UNDULATOR *

D.M. MILLS and P.J. VICCARO

Argonne National Laboratory, 9700 South Cass Avenue, Argonne, IL 60439, USA

A. MERLINI, Q. SHEN and K. FINKELSTEIN

Cornell High Energy Synchrotron Source, Cornell University, Ithaca, NY 14853, USA

The horizontal and vertical emittance of the Cornell Electron Storage Ring (CESR) was measured using the radiation emitted from a short-period (3.3 cm) 123-pole undulator. Average horizontal and vertical emittances measured by this technique were 80 nm-rad and 1.75 nm-rad, respectively. These compare favorably with the results from a charge-coupled device (CCD) system routinely used at CESR and with the calculated values of 65 nm-rad and ~1 nm-rad for the horizontal and vertical emittances respectively.

1. Introduction

A plot of the transverse source size versus angular divergence of a particle beam in a storage ring yields contours of equal particle density that lie on ellipses [1]. These so called phase space plots are parametrized by a property called the emittance, which is equal to the area of the phase space ellipse divided by π. Although the shape and orientation of the ellipse many vary as a function of the particle's position around the ring, the emittance is a constant of the motion. Therefore, the emittance is a fundamental property of the storage ring lattice and accurate measurement of the emittance is an important parameter when comparing the calculated and actual characteristics of particle accelerators.

Because of the push for low-emittance synchrotron radiation storage ring sources (for high-brilliance photon beams), there is considerable interest in developing expertise in measuring the angular and spatial properties of particle beams. The very small beam dimensions and divergences encountered in these low-emittance sources will require modifications to the conventional techniques of measuring beam emittances. For instance, a typical technique for measuring the beam emittance at high-energy-physics storage rings involves using the visible radiation from a dipole or bending magnet source. However, at the 7 GeV Advanced Photon Source (APS), the verticular angular divergence of the positron beam at a bending magnet source is projected to be 7 μrad (for $\beta = 17$ m); this is about a tenth of the natural opening angle ($1/\gamma$) of the emitted radiation, and hence the measurement would be overwhelmed by the natural opening angle of the radiation, and the contribution due to the particle beam emittance would be difficult to determine. One method to minimize the contribution of the radiation opening angle is to make the measurement on an undulator beamline, where the opening angle of the radiation at the odd harmonics is given by

$$(1/\gamma)\left[(1 + K^2/2)/2kN\right] = \sqrt{(\lambda/L)}\,.$$

Here K is the magnetic deflection parameter, k the harmonic number of the emitted radiation, N is the number of periods, λ is the X-ray wavelength and L is the length of the insertion device. For a "typical" insertion device several meters long and a fundamental X-ray wavelength of 1 Å, the radiation vertical opening angle is approximately 10 μrad, comparable to the particle beam divergence.

This approach was taken to measure the emittance at the Cornell Electron Storage Ring (CESR) during dedicated operation for the APS/CHESS undulator [2] run. The goal of these measurements were twofold: to measure the horizontal and vertical emittances of CESR operating in "low emittance" mode, and to investigate the dependence of the emittance on the stored beam current.

2. Experimental technique

Two experimental approaches were considered in the emittance measurements; a fixed/scanning two-slit

* Work supported by the U.S. Department of Energy, Office of Basic Energy Sciences, Division of Materials Sciences, under contract no. W-31-109-ENG-38, and by the National Science Foundation under contract no. DMR-87-19764

0168-9002/90/$03.50 © 1990 – Elsevier Science Publishers B.V. (North-Holland)

measurement and a scanning/scanning two-slit measurement. In the fixed/scanning technique, the first fixed slit acts as the aperture of a pinhole camera and the source is imaged at the hutch. The size of the image can then be measured with a second scanning slit. (Measurement of the image size can also be done by densitometry of the image on a film or with a one-dimensional detector.) With knowledge of the β function, the source properties can be determined from the size of the imaged source [3]. We chose the scanning/scanning two-slit technique. This method involves rastering both slits, but requires no prior knowledge of the accelerator's properties. Unfortunately, because both slits have to be scanned, the data acquisition time is longer than for the fixed/scanning slit technique.

The scanning/scanning two-slit technique for measuring particle beam phase space has been reviewed by Van Steenberger [4], and we will use his notation in this manuscript. We will define $\rho(x, x', y, y')$ as the projection of the six-dimensional phase space density for a particle beam traveling along the z direction. The function ρ has the property that integration over the variables yields the total number of particles N in the beam, i.e.:

$$N = \int\int\int\int \rho(x, x', y, y')\, dx\, dx'\, dy\, dy'. \quad (1)$$

We can also define integrated partial density functions by:

$$D(x, x') = \int\int \rho(x, x', y, y')\, dy\, dy'; \quad (2a)$$

$$D(y, y') = \int\int \rho(x, x', y, y')\, dx\, dx'. \quad (2b)$$

The two parts of eq. (2) give the horizontal and vertical phase space functions of the particle beam.

Now consider two narrow slits, A and B, located Z_a and Z_b from the source and positioned at some point X_a and X_b from the center line (see fig. 1). When the two slits are projected back onto the phase space of the source using the standard matrix transformations for drift spaces,

$$\begin{bmatrix} x_1 \\ x_1' \end{bmatrix} = \begin{bmatrix} 1 & Z_a \\ 0 & 1 \end{bmatrix} \begin{bmatrix} X_a \\ x' \end{bmatrix} \quad (3a)$$

$$\begin{bmatrix} x_1 \\ x_1' \end{bmatrix} = \begin{bmatrix} 1 & Z_b \\ 0 & 1 \end{bmatrix} \begin{bmatrix} X_b \\ x' \end{bmatrix}, \quad (3b)$$

they select a unique point on the source phase space ellipse given by

$$x_1 = (X_a Z_b - X_b Z_a)/(Z_b - Z_a)$$

and

$$x_1' = (X_b - X_a)/(Z_b - Z_a). \quad (4)$$

Similar relationships hold for y and y'. (A comment on notation is appropriate here. The horizontal and vertical beam properties are measured separately, with two sets of horizontal slits and two sets of vertical slits, respectively. Horizontal slits are apertures that limit the horizontal extent of the beam and are used to measure the horizontal beam properties; the vertical slits function similarly.)

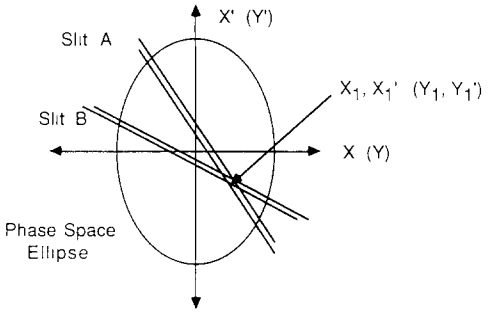

Fig. 1 The projection of the two slits onto the source phase space. Data is collected by first fixing slit A and then recording the measured intensity as slit B is stepped. Slit A is then moved and the procedure repeated until the entire phase space area has been rastered over For a given position of slit A, X_A, and slit B, X_B, the point x_1, x_1' in phase space is sampled.

By recording the X-ray intensity that passes through the two slits, the entire function $D(x, x')$ or $D(y, y')$ can then be mapped out by repeatedly positioning the first slit and scanning the second slit. Note that because we are using slits, the integrations in eq. (2) are automatically performed in the measurement, and alignment of the slits is not as critical as in the case of crossed-slit or pinhole measurements.

All measurements described here were made using monochromatic radiation with CESR running at 5.43 GeV. The monochromator, consisting of two water-cooled Si(311) crystals in a non-dispersive geometry, was adjusted to diffract the first harmonic of the undulator (see fig. 2 for a schematic of experimental arrangement). Initial measurements were made at very low stored currents (< 2 mA in seven-bunch mode) to ensure that the first optical component was not thermally

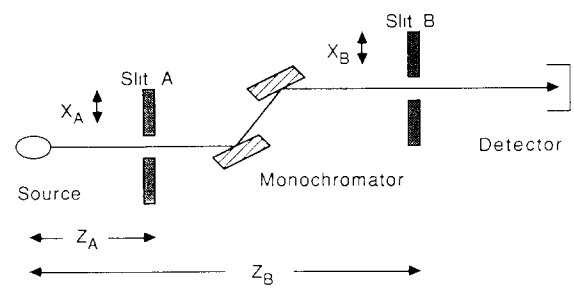

Fig. 2. Schematic of the experimental arrangement for emittance measurements The distances from the source to slit A and slit B were 18.54 and 25 97 m respectively Slit sizes, a, were 100 μm for the horizontal emittance measurements and 25 μm for the vertical emittance measurements

Table 1
Contributions to measured divergence and source size

Term	Source	Expression	Horizontal	Vertical
σ_{par}	beam emittance	$\sqrt{\epsilon\beta}$	1.125 mm	0.070 mm
σ_{dis}	dispersion	$\eta(\sigma_\epsilon/E)$	0.015 mm	0.000 mm
σ_{rad}	radiation	$(1/4\pi)\sqrt{\lambda L}$	0.001 mm	0.001 mm
σ_{slt}	slit size	$a/\sqrt{(2\pi)}$ [a]	0 040 mm	0.010 mm
σ'_{par}	beam emittance	$\sqrt{(\epsilon/\beta)}$	0.058 mrad	0 014 mrad
σ'_{dis}	dispersion	$\eta'(\sigma_\epsilon/E)$	0.045 mrad	0.000 mrad
σ'_{rad}	radiation	$\sqrt{(\lambda/L)}$	0.009 mrad	0.009 mrad
σ'_{slt}	slit size	$(a/Z_a)(1/\sqrt{2\pi})$ [a]	0.002 mrad	0.0005 mrad

[a] Approximation of a square function with a Gaussian function.

strained. Thermal strains could cause an increase in the angular spread of the output beam and hence an error in our emittance determination. To measure the emittance under higher beam currents and still maintain relatively low thermal loads on the monochromator, large currents were stored in a single bunch rather than the standard seven bunches. In this way a large total currents, say 35 mA, could be simulated by having only 5 mA of beam in the storage ring. Implicit in this simulation is the assumption that any growth in beam emittance is due to *intra*bunch interactions and not to *inter*bunch phenomena.

3. Contributions to the measured phase space

Numerous contributions to both the measured source size and source divergence must be removed in order for the true particle beam emittance to be determined. In this work we will assume that the individual contributions can be added in quadrature (although they may not all be Gaussian in nature). The measured source size and divergence (σ_m and σ'_m respectively) can be written for either the horizontal and vertical directions as:

$$\sigma_m^2 = \sum_j \sigma_j^2;\ \sigma_m'^2 = \sum_i \sigma_i'^2. \qquad (4)$$

Tables 1–3 give the explicit form for each σ_i and σ_i' and their numerical values. As can be seen from table 1, the finite slit width has little effect on the measured source size and divergence; the dominant contribution comes from the particle beam emittance, i.e., $\sigma_{particle}$ and $\sigma'_{particle}$.

Table 2
Calculated values of storage ring parameters

Parameter	Horizontal	Vertical
ϵ (m-rad)	6.5×10^{-8}	1.0×10^{-9}
β (m)	19 48	4.89
β'	0.335	0.118
η (m)	−0.022	0.00
η'	0.065	0.00
σ_ϵ/E	6.97×10^{-4}	$6\ 97\times10^{-4}$

4. Analysis of the experimental data

A total of four runs in single-bunch mode were carried out to determine the horizontal emittance: three were at low currents (1–5 mA) and one at a higher current (25–30 mA). The high-current run was the least reliable because of fluctuations and instabilities in the beam position. Because of beam-position instabilities only one low-current, single-bunch measurement of the vertical emittance was acceptable. All runs were made with an undulator magnet gap of 2.4 cm ($K = 0.54$) on the peak of the fundamental ($E = 7.2$ keV), with the exception of one horizontal emittance run, which was made at the third harmonic ($E = 17$ keV) with a magnet gap of 1.8 cm ($K = 0.98$). Two methods, called intensity scaling (IS) and Gaussian fit (GF), were used to analyze the experimental data and are outlined below.

4.1. Intensity scaling

Consider, for example, the horizontal case, and the following upright Gaussian distribution centered at the

Table 3
Physical dimensions

Parameter	Value
$a_{horizontal}$	0.100 mm
$a_{vertical}$	0 025 mm
Z_a	18.54 m
Z_b	25.97 m

origin of the coordinate axes x, x':

$$I(x, x') = I_0 \exp - \left[\frac{x^2}{2\sigma_x^2} + \frac{x'^2}{2\sigma_{x'}^2} \right], \tag{6}$$

where I_0 is the peak intensity measured when the positions of both A and B slits are positioned on the source central ray, and $I(x, x')$ is the measured intensity at the phase space point (x, x'), corresponding to a generic position of the two slits (see eq. (3)). By choosing various intensity levels on the experimental curves, together with the relative slit coordinates X_A and X_B, the corresponding phase space coordinates are calculated. All the points (x_s, x_s') defined as

$$x_s \frac{x}{\sqrt{2 \ln(I_0/I)}}, \; x_s' = \frac{x'}{\sqrt{2 \ln(I_0/I)}} \tag{7}$$

should lie on a ellipse with axes σ_x and $\sigma_{x'}$ in the (x, x') plane, i.e.,

$$\left(\frac{x_s}{\sigma_x}\right)^2 + \left(\frac{x_s'}{\sigma_{x'}}\right)^2 = 1. \tag{8}$$

The intensity scaling procedure defined by eq. (7) is general, i.e., it applies to any Gaussian distribution, which may be tilted or translated relative to the coordinate axes x and x'. The resulting expression, which takes the place of eq. (8), is then a quadratic equation describing a tilted or translated ellipse. A plot of x_s vs x_s' is illustrated in fig. 3a for one of the horizontal emittance measurements. Fig. 4 is a similar plot for the vertical case. The ellipses, chosen by trial and error, are the best visual fit to the points. All the ellipses are upright; small tilts (less than 2°) were not significant,

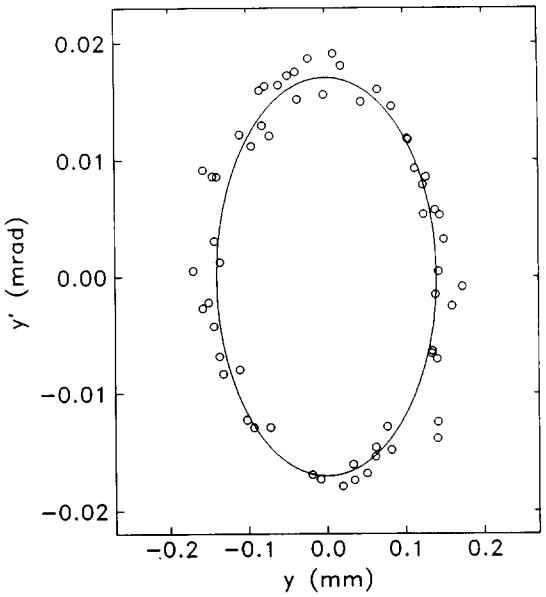

Fig. 4. The vertical phase space data plotted using the intensity scaling (IS) analysis technique taken at 1.7 mA using 7.2 keV X-rays. The measured (uncorrected) 1σ values for the vertical beam size and divergence were 0.14 mm and 0.017 rad respectively.

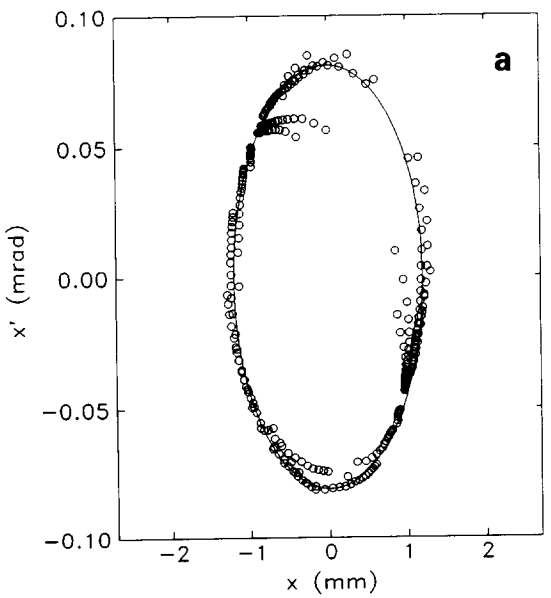

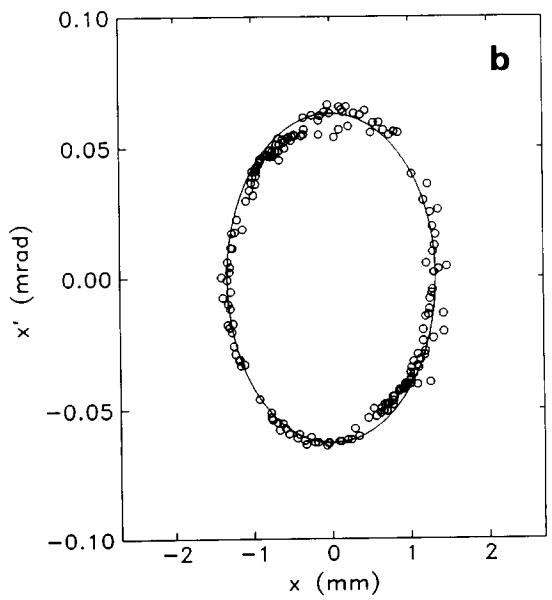

Fig. 3 (a) The horizontal phase space data plotted using the intensity scaling (IS) analysis technique. The data were collected with 1 mA of beam in the storage ring using 17 keV X-radiation from the undulator. The measured (uncorrected) 1σ values for the horizontal beam size and divergence were 1.20 mm and 0.080 mrad respectively. (b) The horizontal phase space plotted using Gaussian fit (GF) analysis procedure. The data were collected with 2 mA of beam in the storage ring using 7.2 keV X-rays. The measured (uncorrected) 1σ values for the beam size and divergence for this case were 1.33 mm and 0.062 mrad respectively.

being well within the experimental errors and the precision of the distances Z_a and Z_B. This result is a confirmation that the derivative of the beta function is nearly zero at the undulator position.

4.2. Gaussian fit

A computer program was also used to obtain a two-dimensional Gaussian fit of the experimental scans after conversion of the slit positions and distances to phase space coordinates. The values of σ_m and σ_m' were extracted from such a fitting. In addition to these two parameters, the program yielded four additional parameters: peak intensity, phase space origin and tilt of the Gaussian distribution. The program iterated the calculation to yield a minimum χ^2 value. The fitting could also reflect an averaging over the crossed area (the experimental window) of the A and B slits. Fig. 3b shows the data analyzed in this fashion.

5. Results

Tables 4 and 5 give the results of the above data analysis and, for comparison, the data obtained in the visible range with a CCD [5]. A comparison between the results of the CCD optics and scanning slits methods warrants the following comments. The agreement between the horizontal emittance results is satisfactory when the values of the source size and the divergence are compared. On the other hand, in the vertical direction, the value of the source size (and hence the emittance) obtained with the scanning slits methods is twice as large as that measured by means of the CCD optics. Such a large discrepancy might be explained by errors arising mainly from the estimate of the optical system resolving power and/or from fluctuations of beam position during the measurements done with scanning slits. The resolving power of the CCD optical system was estimated to be 150 μm – twice the given source-size value. The presence of fluctuations in the beam position during most, if not all, of the slit scans was confirmed by using a highly sensitive beam position monitor. While the beam was stable in the millisecond–second time range, fluctuations with a total excursion of 30–40 μm and a periodicity of about 4 min were observed together with a slow beam drift over a time range of a few hours. Such fluctuations certainly affected the scanning slit measurements, which required 40–45 min, and would result in an apparent increase in source size. The combination of these two sources of error is sufficient to bridge the gap between the two values of the source size.

Acknowledgements

The authors would like to thank all the members of the Argonne National Laboratory, CHESS and CESR staffs who participated in the undulator work during

Table 4
Horizontal emittance

Method	σ_m [mm]	σ_m' [mrad]	σ_{par} [mm]	σ_{par}' [mrad]	Emittance (nm rad)	Conditions
IS	1.33	0.062	1.33	0.042	55	2 mA, $E_{X\text{-}ray} = 7.2$ keV
GF	1.33	0.063	1.33	0.042	55	
IS	1.20	0.080	1.20	0.065	79	1 mA, $E_{X\text{-}ray} = 17$ keV
GF	1.22	0.08	1.22	0.069	83	
IS	1.33	0.058	1.33	0.036	47	25–30 mA, $E_{X\text{-}ray} = 7.2$ keV
CCD optics			1.22	0.061	75	low currents
Calculated			1.13	0.058	65	low currents

Table 5
Vertical emittance

Method	σ_m [mm]	σ_m' [mrad]	σ_{par} [mm]	σ_{par}' [mrad]	Emittance [nm rad]	Conditions
IS	0.14	0.017	0.14	0.014	1.96	1.7 mA, $E_{X\text{-}ray} = 7.2$ keV
GF	0.16	0.018	0.16	0.015	2.40	
CCD optics			0.067	0.014	0 94	low currents
Calculated	0.071	0.016	0.070	0.014	~1	low currents

May 1988. D.M.M. and P.J.V. would like to thank Dr. George Brown of the Stanford Synchrotron Radiation Laboratory for his useful discussions on emittance measurements. D.M.M. would also like to thank the John Simon Guggenheim Foundation for support during this period.

References

[1] A.P. Banford, The Transport of Charged Particles (Spon, London, 1966).

[2] D.H. Bilderback, B.W. Batterman, M.J. Bedzyk, K. Finkelstein, C. Henderson, A. Merlini, W. Schildkamp, Q. Shen, J. White, E.B. Blum, P.J. Viccaro, D.M. Mills, S. Kim, G.K. Shenoy, K.E. Robinson, F.E. James and J.M. Slater, Rev. Sci. Instr. 60 (1989) 1419.

[3] G. Brown, J. Cerino, A. Hoffmann, R. Liu, T. Troxel, P. Wang, H. Wiedemann, H. Winick, M. Berndt, R. Brown, J. Christensen, M. Donald, B. Graham, R. Gray, E. Guerra, C. Harris, C. Hollosi, T. Jones, J. Jowett, P. Morton, J.M. Paterson, R. Pennacchi, L. Riuken, T. Taylor, F. Turner and J. Turner, Proc. 1987 IEEE Particle Accelerator Conf., Washington, DC, eds. E.R. Lindstrom and L.S. Taylor, p. 461.

[4] A. Van Steenberger, Nucl. Instr. and Meth. 51 (1967) 245

[5] S.V. Milton, M.S. Thesis, Cornell University (1988) unpublished.